Check for updates

Original Research Article

Glabridin as a Potential Therapeutic Agent for COPD: Mechanistic Insights into JAK1/STAT1 Pathway Inhibition

Pharmacognosy Magazine
22(3) 885–897, 2026
© The Author(s) 2025
Article reuse guidelines:
in.sagepub.com/journals-permissions-india
DOI: 10.1177/09731296251325348
journals.sagepub.com/home/phm



Weiwei Yuan[1], Hongtao Tan[2], Huihui Li[1], Junxian Chen[3] and Jun Qiu[4]

Abstract

Background: Chronic obstructive pulmonary disease (COPD) is a common inflammatory disorder that is significantly aggravated by tobacco smoke exposure.
Objectives: This study aimed to explore the effect of glabridin (Glab) on the inflammatory response and explain the molecular mechanism of Glab *in vitro* model of human bronchial epithelial cells (16HBE) induced by cigarette smoke extract (CSE).
Materials and Methods: We constructed an *in vitro* model of COPD using CSE induction of 16HBE and applied Glab with differential concentration gradients to the model. Cell viability was assessed using the Cell Counting Kit-8 method. We also measured the apoptosis rate and the release level of inflammatory factors under each simulated condition, mainly based on flow cytometry, enzyme-linked immunosorbent assay, and Western blotting to evaluate the above parameters. Network pharmacology and molecular docking analyses were employed to predict Glab's interactions with the Janus Kinase 1 (JAK1)/signal transducer and activator of transcription 1 (STAT1) signaling pathway. These predictions were subsequently validated via gene knockdown experiments.
Results: Glab can reduce the negative effects of CSE on cells by inhibiting the expression of inflammatory factors. The effect of Glab was concentration-dependent. Molecular docking demonstrated Glab's strong binding affinity for JAK1 at residues GLY263, GLY440, and ASN465. Glab treatment inhibited JAK1/STAT1 phosphorylation, and STAT1 knockdown abrogated Glab's protective effects, confirming its target-specific action.
Conclusion: These findings highlight Glab's potential as an anti-inflammatory agent for COPD by targeting the JAK1/STAT1 signaling pathway. Further studies are warranted to explore its clinical applicability in COPD management.

Keywords

Chronic obstructive pulmonary disease, glabridin, JAK1/STAT1 pathway, molecular docking, network pharmacology

Received 08 January 2025; **revised** 06 February 2025; **accepted** 19 February 2025

Introduction

Chronic obstructive pulmonary disease (COPD) is a common chronic illness, with the clinical pathological feature of airflow obstruction (Hizawa, 2024; Kodaka et al., 2023). It is a chronic inflammatory lung disease and may develop into pulmonary heart disease and respiratory failure. It is now widely acknowledged as a significant global public health challenge (Christenson et al., 2022). In 2019, data released by the World Health Organization indicated that COPD had become the third leading cause of death worldwide. Recurrent episodes of COPD often require hospitalization, increasing the disease burden on society and seriously threatening people's lives and health. Therefore, the discussion of COPD prevention and treatment measures has been increasingly emphasized by scholars at home and abroad.

Based on the available studies, chronic inflammation is the principal pathogenic factor of COPD (Ritchie & Wedzicha, 2020). Macrophages, neutrophils, and other inflammatory

Weiwei Yuan and Hongtao Tan are considered to be co-first authors.
[1]Department of Respiratory, Huizhou Hospital of Guangzhou University of Chinese Medicine (Huizhou Hospital of Traditional Chinese Medicine), Huizhou, Guangdong, China
[2]Department of Traditional Chinese Medicine, Huizhou Central People's Hospital, Huizhou, Guangdong, China
[3]First Faculty of Clinical Medicine, Guangzhou University of Chinese Medicine, Guangzhou, Guangdong, China
[4]Department of Respiratory, Guangzhou Hospital of Integrated Traditional and Western Medicine, Guangzhou, Guangdong, China

Corresponding author:
Jun Qiu, Department of Respiratory, Guangzhou Hospital of Integrated Traditional and Western Medicine, No. 87, Yingbin Avenue, Huadu District, Guangzhou, Guangdong 510800, China.
E-mail: jun__qiu@sina.cn

Creative Commons Non Commercial CC BY-NC: This article is distributed under the terms of the Creative Commons Attribution-NonCommercial 4.0 License (http://www.creativecommons.org/licenses/by-nc/4.0/) which permits non-Commercial use, reproduction and distribution of the work without further permission provided the original work is attributed as specified on the SAGE and Open Access pages (https://us.sagepub.com/en-us/nam/open-access-at-sage).

cells are the main participants in the inflammatory response, and the inflammatory factors they produce directly participate in the inflammatory response observed in COPD (Kapellos et al., 2023). In COPD, airway inflammation is primarily triggered by cigarette smoke exposure, which subsequently activates inflammatory cells, including macrophages, monocytes, and neutrophils. This will subsequently lead to a significant upregulation of representative inflammatory factors such as interleukin-6 (IL-6), interleukin-1β (IL-1β), interleukin-8 (IL-8), and tumor necrosis factor-α (TNF-α) (Aslani et al., 2023; Song et al., 2023). The elevated production of these pro-inflammatory factors exacerbates the inflammatory response. Research has shown that the levels of IL-6, IL-8, and TNF-α in the bloodstream of smoking COPD patients are significantly higher compared to non-smokers (Deveci et al., 2010). Additionally, the severity of airflow limitation correlates positively with the concentrations of these inflammatory markers (Ran et al., 2019), highlighting their clinical significance. Therefore, the modulation of inflammation is a critical therapeutic strategy in the management of COPD. In response to this pathogenic mechanism, by slowing down the underlying inflammatory process and improving the lung function of patients, it may be possible to alleviate their symptoms and enhance their quality of life.

Glabridin (Glab) is a traditional Chinese medicine component isolated from the roots of *Glycyrrhiza* (Fabaceae family) plants and belongs to the isoflavone class (Wahab et al., 2021). Glab is also considered a phytoestrogen, and its biological activities include not only antioxidant properties, scavenging of oxygen free radicals, anti-inflammatory effects, inhibition of capillary permeability, anti-bacterial action, inhibition of tyrosinase activity, adrenocortical hormone-like effects, and anti-allergic reactions but also neuroprotection, anti-atherosclerotic effects, and so on (Guo et al., 2022; Li et al., 2023; Parlar et al., 2020; Tan et al., 2022; Zhang et al., 2022). Previous research has shown that Glab significantly inhibits the secretion of inducible prostaglandin E2, IL-6, IL-8, nitric oxide, and TNF-α (Zhan et al., 2023). Further investigations have revealed that Glab mitigates inflammatory responses and displays antioxidant properties by inhibiting the extracellular signal-regulated kinase (ERK) and mitogen-activated protein kinase 14 (p38MAPK) signaling pathways, thereby alleviating lipopolysaccharide (LPS)-induced lung injury in rats (Zhang et al., 2017). There have been numerous research reports on the biological activities of Glab, and its antioxidant, anti-inflammatory, and capillary permeability-inhibiting effects align well with the pathophysiological mechanisms of lung injury. However, to date, no studies have analyzed the relationship between Glab and COPD.

Based on previous studies, we aim to explore the potential impact of Glab on the inflammatory response of human bronchial epithelial cells (16HBE) induced by cigarette smoke extract (CSE) and uncover the underlying mechanism based on network pharmacology prediction and experimental verification.

Materials and Methods

Bioinformatics Analysis

Drug target acquisition databases were introduced to analyze target genes in Glab, including Traditional Chinese Medicine Systems Pharmacology Database and Analysis Platform (TCMSP) (http://lsp.nwu.edu.cn/tcmsp.php), STITCH (http://stitch.embl.de/), and Swiss Target Prediction (http://old.swisstargetprediction.ch/) databases. Disease target acquisition databases were introduced to analyze target genes in COPD, such as BATMAN-TCM (http://bionet.ncpsb.org.cn/batman-tcm/#/home), DisGeNET (https://www.disgenet.org/) databases, OMIM (https://omim.org/), and DrugBank (https://go.drugbank.com/). The overlapping targets between Glab and COPD were determined using Venn diagrams generated via R language. Cytoscape (version 3.7.0) was utilized to construct relevant target-pathway network maps for Glab in the context of COPD. Gene Ontology (GO) and Kyoto Encyclopedia of Genes and Genomes (KEGG) analyses were conducted to elucidate pathways, associated enzymes, and gene metabolism products. Additionally, BLAST alignment was used to retrieve pathway information for gene sequences. Functional annotations of hub genes based on GO and KEGG were performed using DAVID online tools (https://david.ncifcrf.gov/).

CSE Preparation

We procured three filter-tipped cigarettes that adhere to the 3R4F standard, with each cigarette containing 9.5 mg of tar and 0.73 g of nicotine. Utilizing a 50 mL syringe, we extracted 30 mL of phosphate-buffered saline. The cigarettes underwent a consistent aspiration process for 4 min. Post-combustion of a single cigarette, the resultant solution had its pH meticulously adjusted to the alkaline range of 7.2–7.4 employing a 1 molar solution of sodium hydroxide. Subsequently, the solution underwent sterilization via filtration through a 0.45 μM membrane equipped with a filter head. Before measurement, precise calibration should be carried out first, and the absorbance (OD) of the solution should be adjusted at a wavelength of 320 nm. The CSE obtained is to be conserved at an ultra-low temperature of –80°C. Prior to utilization in experiments, it should be rapidly thawed and expeditiously used within a 30-min window to ensure the integrity and reactivity of the components for the study.

Cell Culture and Grouping

16HBE were sourced from Sigma (catalog number: SCC150, USA) and cultured according to established protocols. We transferred the cells to Dulbecco's Modified Eagle Medium (DMEM) and added 10% fetal bovine serum (containing 10,000 units/L penicillin, 2 mmol/L glutamine, and 10 mg/L

streptomycin). Cultivation was conducted at 37°C with 5% CO_2. Cell growth was closely monitored, and subculturing was performed every 2 weeks. Cells in the logarithmic growth phase were utilized for experimental studies. To examine the effects of varying concentrations of Glab (1.25, 2.5, 5, 10, and 20 μM; CAS number: 59870-68-7, supplier: Sigma-Aldrich, USA) on 16HBE cells, a 24-h treatment regimen was applied. We needed to measure cell viability. We used the Cell Counting Kit-8 (CCK-8) method to determine the cell viability of the COPD *in vitro* cell model and assess the impact of different environments on 16HBE cells. We placed 16HBE cells in five different growth environments: (a) Control group; (b) CSE exposure group; (c) CSE + 2.5 μM Glab group; (d) CSE + 5 μM Glab group; and (e) CSE + 10 μM Glab group. For the experimental group exposed to CSE, we observed the cell growth at regular intervals. When the cell confluence reached 80–90%, we transferred them to the DMEM medium. Then, a growth environment with 2% CSE was established to simulate the inhalation of CSE and continue the culture. After the CSE model was established, 2.5, 5, or 10 μM of Glab was added to the medium, respectively, as the CSE + Glab groups. Each group was co-incubated for 24 h continuously. In addition, to explore the relationship between Glab and the Janus kinase 1 (JAK1)/signal transducer and activator of transcription 1 (STAT1) signaling pathway, we used the oxygen-glucose deprivation/reoxygenation (OGD/R) model for subsequent experiments. We set up four different experimental conditions for the subsequent experiments, namely: (a) siNC + DMSO group; (b) siSTAT1 + DMSO group; (c) DMSO + Glab group; and (d) siSTAT1 + Glab group. For the siNC + DMSO group, DMSO (0.05%) treatment was given after transfection of siNC in 16HBE cells exposed to CSE. In the experimental group designated siSTAT1 + DMSO, the administration of DMSO (0.05%) occurred subsequent to the transfection of siSTAT1 in 16HBE cells that had been exposed to CSE. In the group designated siNC + Glab, the administration of Glab (5 μM) occurred subsequent to the transfection of siNC in 16HBE cells that had been exposed to CSE. For the siSTAT1 + Glab group, 16HBE cells transfected with siSTAT1 and exposed to CSE were subsequently treated with Glab (5 μM). Upon completion of the experimental procedures, the cells were harvested for further analysis.

Genetic Knockdown

We developed two siRNA constructs targeting STAT1, designed to optimize knockdown efficiency and minimize off-target effects (Qiagen, Germany). Selected siRNAs were incorporated into the pLKO.1 vector for stable expression. For transfection, cells were grown to 70% confluence in DMEM with antibiotics, not serum, to prevent complex interference and cell staining. Lipofectamine® 3000 was used for plasmid transfection. Cells were collected under conditions of 5% CO_2 and 37°C for subsequent experiments.

Cell Viability Assay

We used 96-well plates to inoculate 16HBE cells. The cell density on the inoculation plate was 8×10^3. After the designated treatments for each group, we prepared the CCK-8 solution. In each well, we added 10 μL of the above solution. The inoculated plates were incubated at an environmental temperature of 37°C for 30 min. We measured the OD of the cells after culture at 450 nm using a microplate reader. These OD values were used as indicators of cell viability. To calculate the survival rate of cells in each group, the OD values were normalized relative to those of untreated cells cultured in a standard medium, which served as the control.

Cell Apoptosis Assay

After altering the growth environment of the cells, we investigated the impact of different grouping conditions on cell growth by comparing the apoptosis rates of cells in different groups. This step utilized the Annexin V-FITC/PI Cell Apoptosis Detection Kit (Catalog No.: V13242) produced by Invitrogen, USA. All procedures were carried out in accordance with the standard protocol. The prepared buffer was specifically designed for propidium iodide (PI) staining procedures and Annexin V-FITC. A suspension of 1×10^5 16HBE cells was prepared using this buffer for each experiment. This suspension was then incubated in the absence of light at ambient temperature for 1 h. Subsequently, the apoptotic cell count was evaluated utilizing FACS flow cytometry in conjunction with CellQuest software for analysis.

Enzyme-linked Immunosorbent Assay (ELISA)

The cell suspension obtained in the previous step was subjected to centrifugation for layering. The centrifugation was carried out at a radius of 13.7 cm at a speed of 3,000 rpm for 15 min at 4°C. After centrifugation, the cell supernatant and the upper serum layer were observed to be separated, and the two different components were taken out. To assess the degree of the inflammatory response of the cells, the levels of TNF-α, IL-6, and IL-8 needed to be determined. According to the manufacturer's protocol, an ELISA was used to determine the result. Specifically, TNF-α was assessed using a kit from Proteintech Group Inc. (Cat. No. KE10002, Wuhan, China), IL-6 was detected with a kit from Boster Bio (Cat. No. FEK0411, USA), and IL-8 was measured using a kit from G-Biosciences (Cat. No. IT6134, USA).

Quantitative Real-time Polymerase Chain Reaction (qRT-PCR)

From the cell suspension obtained in the previous step of layering, we extracted the total RNA. This step was carried out

using the Trizol reagent kit. We also needed to measure the quality and concentration of the extracted RNA. We used the Nano-300 micro-spectrophotometer to measure and evaluate these parameters. We also needed to generate complementary deoxyribose nucleic acid (cDNA). We used 1 ng of purified RNA extracted as the template for reverse transcription. 1 ng of purified RNA was reverse transcribed into cDNA using the cDNA First Strand Synthesis Kit produced by FastKing. The generated reverse-transcribed DNA will be used in the subsequent qRT-PCR experiment. The generated cDNA will be used as the raw material template for the experiment. For the RT-qPCR reaction, each 20 mL mixture contains 0.4 μL of forward primer, 10 μL of 2 × Supermix, 0.4 μL of reverse primer, 2 μL of cDNA template, 0.4 μL of PASSIVEDYE, and 6.8 μL of nuclease-free water. The experimental conditions for the thermal cycling are as follows: First, the temperature is raised to 95°C to denature the raw materials for 10 min. Then, 40 cycles are repeated, each consisting of maintaining 95°C for 5 s, cooling to 60°C for 30 s, and then heating to 72°C for 30 s. The qPCR based on fluorescence was performed on the CFX96 detection system using the TB Green® Premix Ex Taq™ (Tli RNaseH Plus) reagent kit, with a total reaction volume of 25 mL. The amplified products obtained are the key factors for evaluating the inflammatory response in the subsequent steps and can be directly used to quantify the mRNA expression level. The primer sequences are detailed in Table 1.

Western Blotting

The extracted proteins were further separated and purified by 10% sodium dodecyl sulfate-polyacrylamide gel electrophoresis. The proteins obtained after electrophoresis were transferred onto polyvinylidene fluoride (PVDF) membranes for subsequent experiments, with a protein concentration of 20 μg/mL. Then, the membranes were transferred to the corresponding primary antibodies detailed in Table 2 and incubated at 4°C. The proteins were incubated with the primary antibodies overnight. Subsequently, the PVDF membranes were removed. Horseradish peroxidase (HRP)-conjugated goat anti-rabbit or anti-mouse immunoglobulin G (IgG) secondary antibodies were added. The environmental temperature was adjusted to room temperature. Incubation was carried out for 2 h. Next, it was necessary to detect the protein expression. An enhanced chemiluminescence (ECL) detection system was used. Through this detection system, the various protein bands could be observed, and their intensities were quantified using ImageJ software through grayscale analysis.

Table 1. Primer Sequences.

Gene	Sequence	
JAK1	Forward	TATTGGGTGGCCAGAAGCAG
	Reverse	TGGTCCATAGAGCCATGCAG
STAT1	Forward	AAGTCTGGCAGCTGAGTTCC
	Reverse	TACCACAGGATAGACGCCCA
GAPDH	Forward	GGCAAATTCAACGGCACAGT
	Reverse	GGCCTCACCCCATTTGATGT

Table 2. The Antibodies Used in This Research.

Antibody	Manufacturer	Cat. No.	Dilution
p-JAK1	MyBioSource.com	MBS9244090	1:1,000
JAK1	Boster Bio	M00330-1	1:1,500
STAT1	Boster Bio	M00036-1	1:1,000
p-STAT1	Boster Bio	A00036Y701-2	1:1,500
β-actin	Boster Bio	M01263	1:2,000

Molecular Docking Study

The JAK–STAT signaling pathway contains a key protein, JAK1, whose three-dimensional (3D) structure is sourced from the Protein Data Bank (PDB, http://www.wwpdb.org/). The PDB database is a large online resource that provides researchers with a vast amount of protein structure data. It leads users to a platform where various protein structures can be accessed, offering valuable resources for scientific research. Moving on to the molecular structure of Glab, we procured its 3D coordinates from the SPECS chemical library, a comprehensive database managed by Schrodinger, USA. The SPECS library is renowned for its extensive collection of characterized compounds, which are instrumental in various scientific and medicinal applications. The 3D structure of Glab was refined and prepared for molecular docking studies using the LigPrep module, a component of the Schrodinger software suite. LigPrep is designed to generate 3D structures for ligands, considering various factors such as ionization states and tautomerism, which ensures that the ligand is represented in a biologically plausible form.

Statistical Analysis

All the experimental data obtained in this experiment were analyzed and compared using the statistical analysis software Statistic Package for Social Science (SPSS) 22.0. To ensure that our experimental data results were not random, we conducted at least three independent and repeated experiments for each type of experiment. The data results from the three repeated experiments were averaged and the final experimental data were presented in the form of mean ± standard error. Non-parametric statistical analysis was conducted using the Kruskal–Wallis test. The *t*-test was used for comparisons between groups. One-way analysis of variance (ANOVA) was very suitable for evaluating the differences among multiple groups in this study. p values $< .05$ were considered statistically significant.

Results

Glab Alleviates the CSE-induced Inflammation and Apoptosis in 16HBE Cells

Figure 1A presents the chemical structural formula of Glab, providing a visual foundation for understanding its molecular composition. In this study, based on the 16HBE cell experiment (a highly differentiated normal 16HBE line), we conducted a comprehensive safety assessment of Glab's biological activity. The research results indicated that after treatment with different concentrations of Glab, there was no significant impact on cell viability, thereby confirming the safety of Glab (Figure 1B).

Building on this, we proceeded to simulate smoking exposure by treating 16HBE cells with a specific concentration of CSE. Then, we prepared three concentrations of Glab solutions, namely 2.5, 5, and 10 μM, for subsequent experiments. We applied the prepared Glab solutions to the COPD *in vitro* cell model. Through the CCK-8 detection method, we observed that the 16HBE cells exposed to CSE and treated with Glab had a healthier cell state compared to those without Glab treatment. Encouragingly, intervention with Glab at the aforementioned doses led to a robust and dose-dependent recovery of cellular activity (Figure 1C).

Further investigation into the apoptotic effects was conducted. The data results of flow cytometry indicated that the apoptosis rate of 16HBE cells under the influence of the CSE

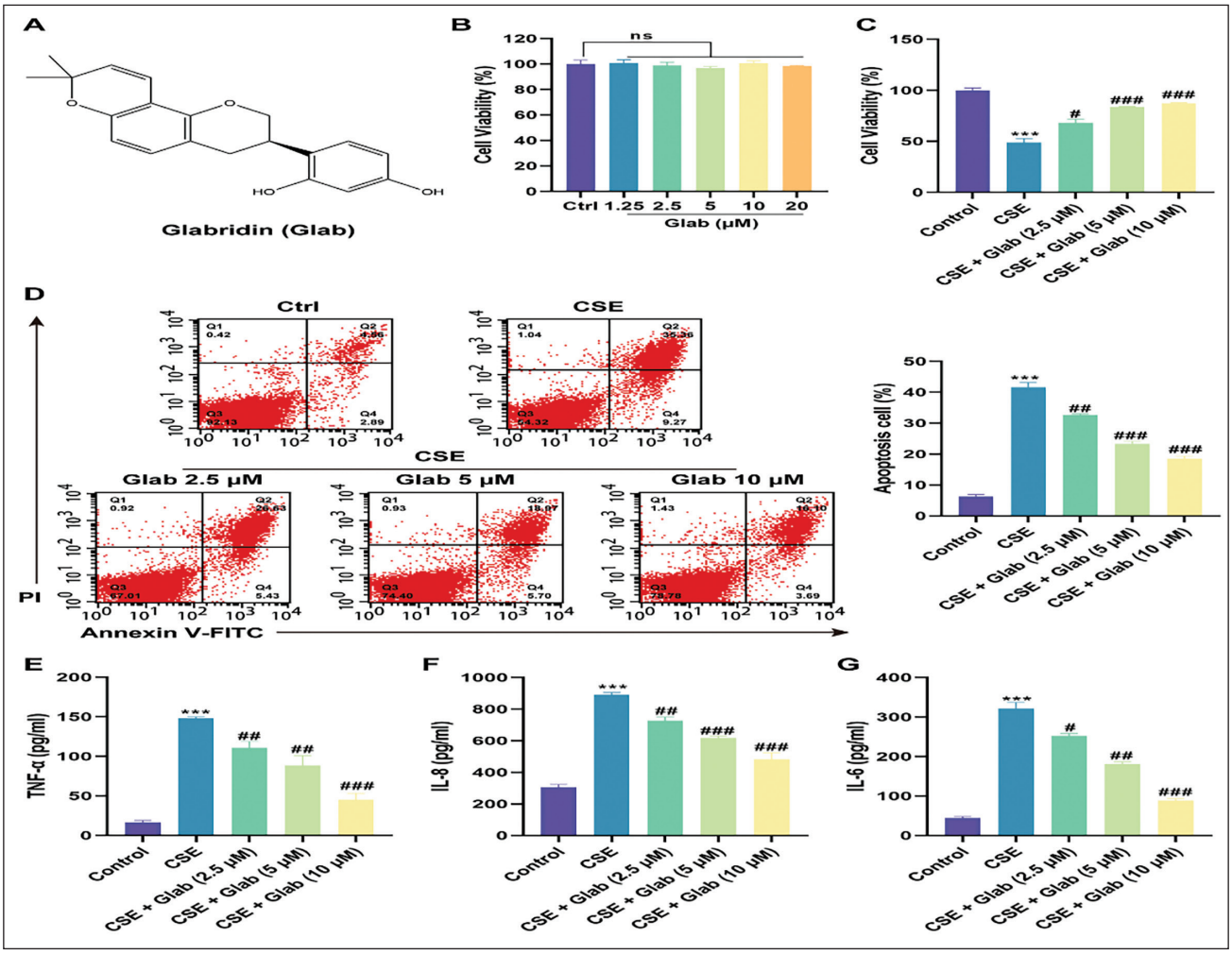


Figure 1. Glabridin (Glab) Alleviates the Cigarette Smoke Extract (CSE)-induced Inflammation and Apoptosis in Human Bronchial Epithelial Cells (16HBE). (A) Chemical Structural Formula of Glab. (B) Cell Counting Kit-8 (CCK-8) Evaluation of Cell Viability of 16HBE Cells Intervened with Glab (1.25, 2.5, 5, 10, and 20 μM). (C) CCK-8 Evaluation of 16HBE Cell Viability Intervened with Glab (2.5, 5, and 10 μM) on the Basis of Exposure to CSE. (D) Annexin V-FITC/PI Double Staining Evaluation of 16HBE Cell Apoptosis Intervened with Glab (2.5, 5, and 10 μM) on the Basis of Exposure to CSE. (E) Enzyme-linked Immunosorbent Assay (ELISA) Evaluation of Tumor Necrosis Factor-α (TNF-α) Contents in 16HBE Cells Intervened with Glab (2.5, 5, and 10 μM) on the Basis of Exposure to CSE. (F) ELISA Evaluation of Interleukin-8 (IL-8) Contents in 16HBE Cells Intervened with Glab (2.5, 5, and 10 μM) on the Basis of Exposure to CSE. (G) ELISA Evaluation of Interleukin-6 (IL-6) Contents in 16HBE Cells Intervened with Glab (2.5, 5, and 10 μM) on the Basis of Exposure to CSE. Data: Mean ± SEM. $n = 3$. $^{***}p < .001$ versus Control Group. $^{\#}p < .05$, $^{\#\#}p < .01$, $^{\#\#\#}p < .001$ versus CSE Group.

environment increased by seven times compared with that of normal cells. However, the health status of 16HBE cells stimulated by CSE improved significantly under the influence of Glab and the apoptosis rate elevated by CSE decreased. Moreover, this biological effect was dose-dependent. As the dosage of Glab increased, the health status of 16HBE cells recovered more obviously (Figure 1D).

Given the established link between the dysregulation of inflammatory factors and the severity, progression, and prognosis of COPD, we extended our study to evaluate the protein content of key pro-inflammatory cytokines in cell supernatants, including TNF-α, IL-8, and IL-6. Our results demonstrated a significant upregulation of TNF-α (Figure 1E), IL-8 (Figure 1F), and IL-6 (Figure 1G) in response to CSE exposure. It is obvious that Glab's intervention can alleviate the enhanced inflammatory response caused by CSE stimulation, thereby improving cell survival treatment, and this biological effect shows a positive dose-dependent relationship. This discovery highlights the potential of Glab as an inflammatory modulator in COPD.

Prediction of the Potential Mechanism of Glab Treatment Against COPD via Network Pharmacology

We further investigated the molecular mechanism of Glab in the treatment of COPD, aiming to identify the protein targets that play an active role in the therapeutic process. Our research employed a two-stage, database-based gene screening method. Initially, we utilized a suite of databases including STITCH, TCMSP and SwissTargetPrediction to identify potential target genes of Glab, culminating in the identification of 182 candidate genes. Second, we conducted a database-driven screening of potential target genes involved in COPD using repositories such as BATMAN-TCM, DrugBank, OMIM, and DisGeNET. This search yielded a total of 707 possible target genes. Following the comprehensive gene screening process, we employed Venn diagrams to graphically represent the intersecting targets of Glab and those implicated in COPD (Figure 2A). Next, we harnessed the power of Cytoscape software to meticulously construct a comprehensive target-pathway network map. This network map encapsulated the 79 intersecting target genes of Glab and COPD, featuring prominent genes such as *Bax*, *MAPK1*, *CNR2*, *AKT1*, *HTR1B*, *BRAF*, and *ABHD6*, among others (Figure 2B). Following this, we performed a detailed enrichment analysis of the GO and KEGG pathways associated with these 79 key genes. The analysis identified several significantly enriched KEGG pathways, such as chemical carcinogenesis-DNA adducts, transforming growth factor (TGF)-beta signaling pathway, and mammalian target of rapamycin (mTOR) signaling pathway (Figure 2C–D). These findings highlight the intricate and interconnected nature of the pathological processes involved in COPD. The key factors within each pathway may serve as potential candidate targets for future therapeutic interventions. Based on the foundation of previous studies, this research has decided to delve deeper into the JAK–STAT signaling pathway. Figure 2E vividly depicts its complex components and interactions.

Glab Regulates the JAK1/STAT1 Axis in CSE-treated 16HBE Cells

The molecular docking analysis revealed that Glab exhibited a strong binding affinity for the JAK1 protein, with key interaction sites identified at GLY263, GLY440, and ASN465 residues (Figure 3A). Other experimental data from this study further verified this finding. We used Western blotting to further support this conclusion. The experimental results showed that the expression of JAK1 and STAT1 signaling pathways in 16HBE cells stimulated by CSE was significantly increased. The mRNA and protein levels of these two pathways were both significantly upregulated. However, after treatment with different concentrations of Glab from low to high, the expression levels of JAK1 and STAT1 gradually returned to near-normal levels. This biological effect was concentration-dependent on Glab (Figure 3B–D). These cumulative results strongly demonstrated that Glab interacts with JAK1 as a potential drug target. As a result, Glab inhibited the expression of the JAK–STAT signaling pathway in the COPD cell model, blocked JAK–STAT activation, reduced the expression of inflammatory factors, and thereby alleviated the inflammatory response.

Knockdown STAT1 Reverses the Protective Effect of Glab in CSE-treated 16HBE Cells

To delve deeper into the mechanism by which Glab confers its protective effects in COPD, we conducted experiments to silence STAT1 in 16HBE cells. As depicted in Figure 4A, the siRNA construct siSTAT1#2 demonstrated a markedly higher inhibition rate of STAT1 protein expression compared to siSTAT1#1. This led us to select siSTAT1#2 for subsequent experiments. Subsequently, we conducted STAT1 knockdown experiments or Glab combined treatment on 16HBE cells after CSE stimulation. The experiments demonstrated that downregulation of STAT1 significantly enhanced cell viability (Figure 4B), reduced cell apoptosis (Figure 4C), and decreased the expression of pro-inflammatory cytokines such as TNF-α (Figure 4D), IL-8 (Figure 4E), and IL-6 (Figure 4F). These findings also indicated that STAT1 knockdown reversed the protective effect of Glab in CSE-treated 16HBE cells. However, when Glab was introduced alongside STAT1 knockdown, no additional significant improvements in cell viability, apoptosis rate, or pro-inflammatory factor expression were observed (Figure 4B–F). These observations suggest that the lack of drug targets for Glab results in its inability to function, which further confirms that the JAK1/STAT1

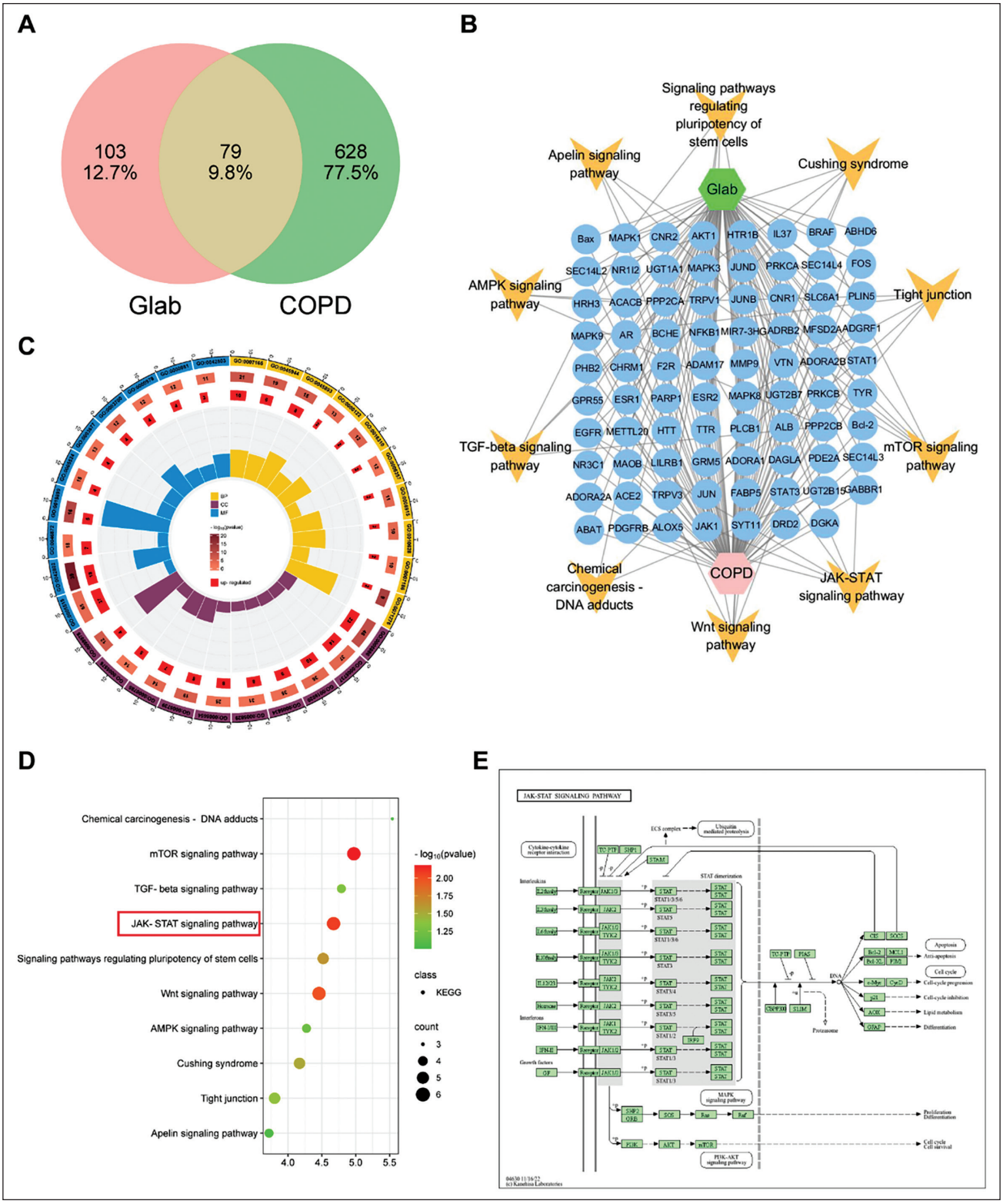


Figure 2. Prediction of Potential Mechanism of Glabridin (Glab) Treatment Against Chronic Obstructive Pulmonary Disease (COPD) via Network Pharmacology. (A) Venn Diagram of Intersecting Targets of Glab and COPD Target Genes Using Venn R Language. (B) Construction of Target-Pathway Network Maps for Glab for COPD Using Cytoscape (3.7.0) Software. (C) Gene Ontology (GO) Enrichment Analysis of 79 Intersecting Targets Using ClusterProfiler R Language Package. (D) Kyoto Encyclopedia of Genes and Genomes (KEGG) Pathway Enrichment Analysis of 79 Intersecting Targets Using ClusterProfiler R Language Package. (E) Retrieval of Specific Regulatory Information for the Janus Kinase (JAK)–Signal Transducer and Activator of Transcription (STAT) Signaling Pathway Based on the KEGG Library.

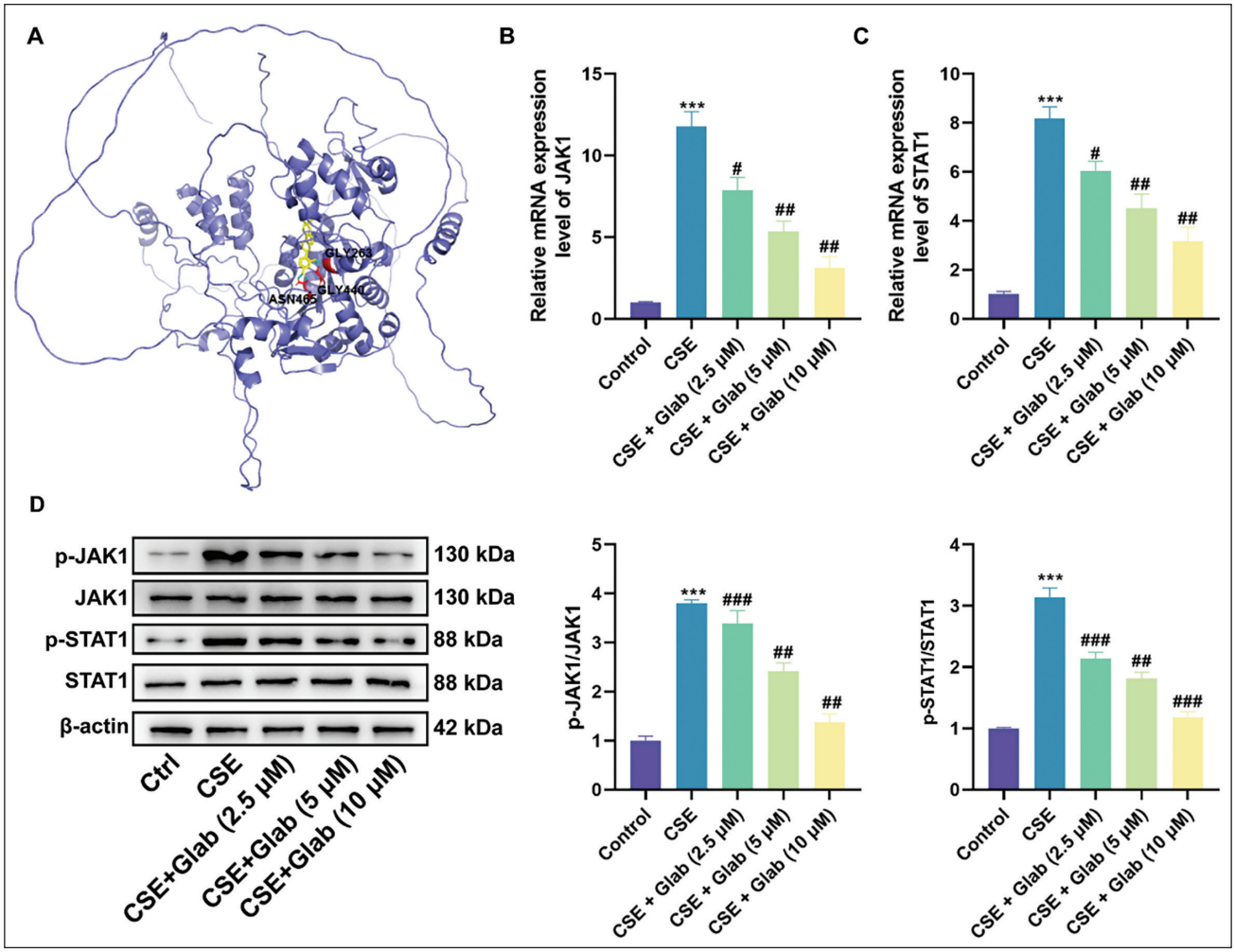


Figure 3. Glabridin (Glab) Regulates the Janus Kinase 1 (JAK1)/Signal Transducer and Activator of Transcription 1 (STAT1) Axis in Cigarette Smoke Extract (CSE)-treated Human Bronchial Epithelial Cells (16HBE). (A) Predicted Molecular Docking Map of the Drug Glab and the Protein JAK1. (B) RT-qPCR Evaluation of JAK1 mRNA Levels in 16HBE Cells Intervened with Glab (2.5, 5, and 10 μM) on the Basis of Exposure to CSE. (C) RT-qPCR Evaluation of STAT1 mRNA Levels in 16HBE Cells Intervened with Glab (2.5, 5, and 10 μM) on the Basis of Exposure to CSE. (D) Western Blot Assay Evaluation of JAK1 and STAT1 Protein Levels in 16HBE Cells Intervened with Glab (2.5, 5, and 10 μM) on the Basis of Exposure to CSE. Data: Mean ± SEM. $n = 3$. ***$p < .001$ versus Control Group. $^{\#}p < .05$, $^{\#\#}p < .01$, $^{\#\#\#}p < .001$ versus CSE Group.

pathway is a mediator that mediates the protective effects of Glab in COPD.

Discussion

COPD is primarily attributed to prolonged exposure to harmful gases, with smoking being the most prevalent causative factor (Upadhyay et al., 2023). During the development of COPD, the first line of immune defense blocks CSE first. The first line of immune defense is bronchial epithelial cells, which are among the earliest cells to be affected by cigarette smoke. The regeneration and proliferation of these epithelial cells are crucial for the repair of damaged tissues (Gao et al., 2015). CSE can simulate the cellular responses caused by smoking. 16HBE cells, as a type of human bronchial epithelial cell, exhibit pathological features similar to those of COPD in a CSE environment (Zhang et al., 2021). Therefore, they were used to construct an *in vitro* model of COPD. We investigated the pharmacological effects of different concentrations of Glab on normal or CSE-stimulated 16HBE cells. The experimental results demonstrated that Glab did not significantly affect cell viability, highlighting its favorable safety profile. Based on these findings, we further investigated the effects of Glab on the viability of 16HBE cells under simulated smoking conditions, the apoptosis of 16HBE cells stimulated by CSE and the various inflammatory pathways. Our research results indicated that the viability of 16HBE cells significantly declined after being stimulated by CSE, the

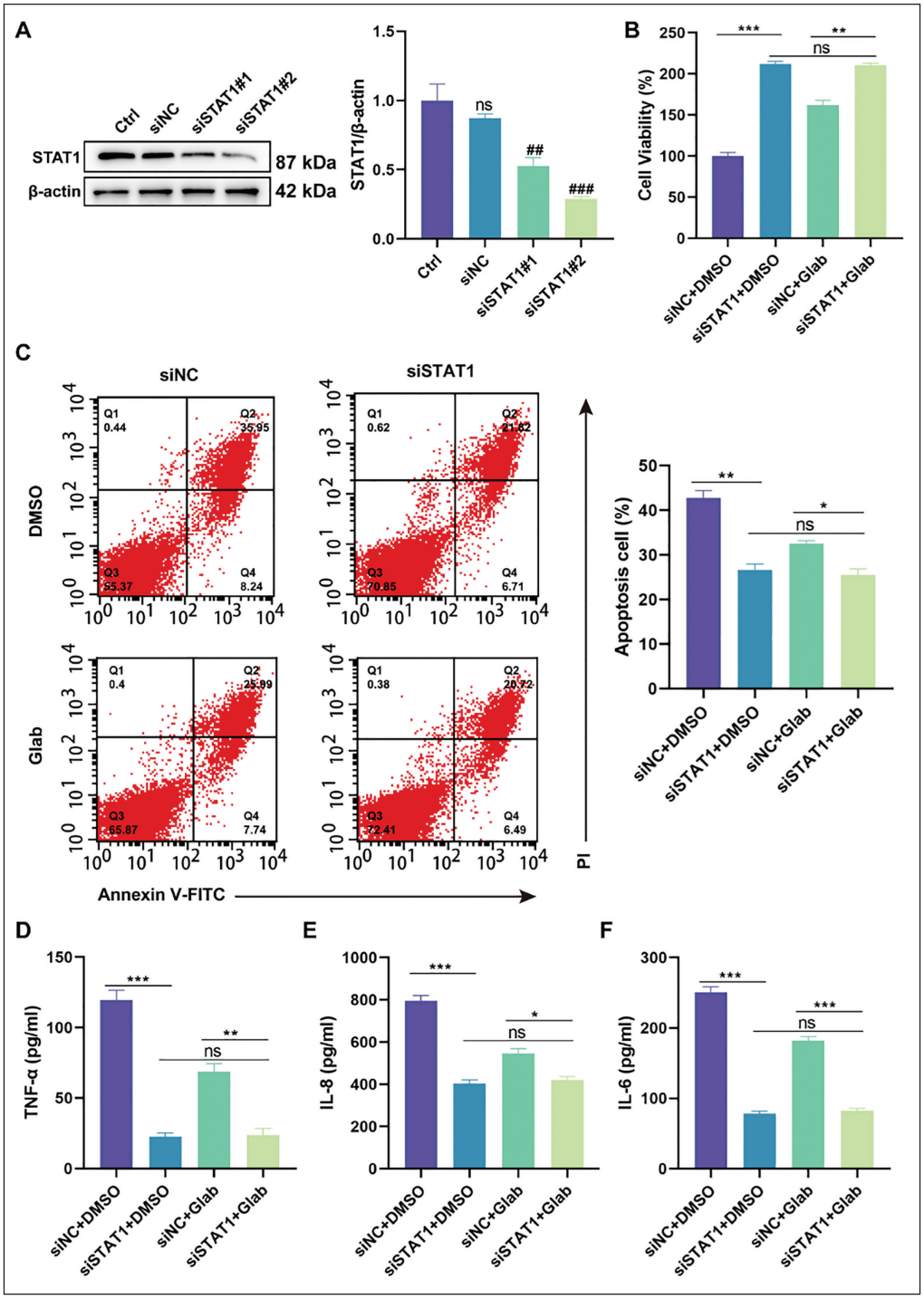


Figure 4. Knockdown Signal Transducer and Activator of Transcription 1 (STAT1) Reverses the Protective Effect of Glabridin (Glab) in Cigarette Smoke Extract (CSE)-treated Human Bronchial Epithelial Cells (16HBE). (A) Western Blot Assay Evaluation of STAT1 Protein Levels in 16HBE Cells Transfected with siSTAT1#1 or siSTAT1#2. $^{ns}p > .05$, $^{\#\#}p < .01$, $^{\#\#\#}p < .001$ versus Control Group. (B) Cell Counting Kit-8 (CCK-8) Evaluation of Viability of 16HBE Cells Transfected with siSTAT1#2 Alone or Administered Glab (2.5, 5, and 10 μM) Therapy Simultaneously on the Basis of Exposure to CSE. (C) Annexin V-FITC/PI Double Staining Evaluation of Apoptosis of 16HBE Cells Transfected with siSTAT1#2 Alone or Administered Glab (2.5, 5, and 10 μM) Therapy Simultaneously on the Basis of Exposure to CSE. (D) Enzyme-linked Immunosorbent Assay (ELISA) Evaluation of Tumor Necrosis Factor-α (TNF-α) Contents in 16HBE Cells Transfected with siSTAT1#2 Alone or Administered Glab (2.5, 5, and 10 μM) Therapy Simultaneously on the Basis of Exposure to CSE. (E) ELISA Evaluation of Interleukin-8 (IL-8) Contents in 16HBE Cells Transfected with siSTAT1#2 Alone or Administered Glab (2.5, 5, and 10 μM) Therapy Simultaneously on the Basis of Exposure to CSE. (F) ELISA Evaluation of Interleukin-6 (IL-6) Contents in 16HBE Cells Transfected with siSTAT1#2 Alone or Administered Glab (2.5, 5, and 10 μM) Therapy Simultaneously on the Basis of Exposure to CSE. Data: Mean ± SEM. $n = 3$. $^{*}p < .05$, $^{**}p < .01$, $^{***}p < .001$.

secretion of pro-inflammatory factors increased, and the apoptosis rate rose markedly. These results suggest that the viability of 16HBE cells decreases under the continuous stimulation of CSE. Subsequently, when 16HBE cells were treated with different concentration gradients of Glab, it was observed that Glab can enhance the recovery of cell viability in a dose-dependent manner. Furthermore, Glab markedly reduced the occurrence of cell apoptosis in response to CSE stimulation, exhibiting a dose-dependent effect. In the pathological process of COPD, abnormal apoptosis can destroy alveolar epithelial cells and alveolar wall structure, thereby promoting the development of emphysema and airflow limitation (Dang et al., 2020).

The development process of COPD can be altered due to the activation of inflammatory factors. To further explore this relationship, we constructed an *in vitro* COPD model. This model was used to simulate the process of how Glab exerts its anti-inflammatory effects and thereby alleviates the damage caused by CSE to cells. Our findings revealed that after being stimulated by CSE, the secretion of pro-inflammatory cytokines such as TNF-α, IL-8, and IL-6 significantly increased. However, since Glab can participate in regulating the expression of various inflammatory factors, it can reduce the inflammatory response and slow down the progression of COPD. Treating with Glab showed that the higher the concentration of Glab, the more pronounced its inhibitory effect on inflammation and the better the therapeutic effect. Its biological effect exhibited a dose-dependent relationship, effectively suppressing the increase of pro-inflammatory cytokines. This biological effect highlights the potential of developing glycyrrhizic acid as a modulator of inflammatory responses in COPD. Glab has diverse biological effects and has shown therapeutic efficacy in various disease processes. Currently, it has been found that Glab can achieve certain effects in anti-inflammatory, antioxidant, and anti-tumor treatments. Among them, studies on lung injury have demonstrated its significant therapeutic potential. For instance, a 2017 study showed that Glab could treat acute respiratory distress syndrome (ARDS). In the LPS-induced ARDS model of this study, the condition was effectively alleviated after Glab treatment. The mechanism involves the inhibition of the p38MAPK/ERK signaling pathway (Zhang et al., 2017). Specifically, Glab reduced the wet-to-dry weight ratio of lung tissue caused by LPS and improved the histopathological features of the lungs (Zhang & Li, 2016). Additionally, Glab is involved in the regulation of the expression of various inflammatory factors. For example, the levels of TNF-α and IL-18 in plasma were inhibited under the influence of Glab, with significant reductions in their expression. Moreover, Glab also regulates the levels of antioxidant and oxidative stress markers in the lungs (Weng et al., 2024; Zhang & Li, 2016). Glab also modulated neutrophil extracellular traps, inhibited cellular focal death, and alleviated sepsis-induced lung injury (Kang et al., 2005). These findings suggest that Glab exerts protective effects against lung injury through multiple mechanisms. In drug delivery systems, a novel carrier for dry powder inhalers sensitive to reactive oxygen species has been reported to act synergistically with drugs like Glab, advancing the study of new excipients for treating and delivering drugs for acute lung injury (ALI) (He et al., 2022). Collectively, our study indicates that Glab is not only safe for 16HBE cells but also demonstrates a protective role against CSE-induced cellular damage. By inhibiting CSE-induced apoptosis and reducing the release of inflammatory factors, Glab seems to have great potential in the treatment of COPD and may become a candidate drug for future treatment.

Elucidating the molecular targets of Glab in COPD represents a significant advancement in understanding the therapeutic potential of this natural compound. Subsequently, this study meticulously designed a two-stage, database-driven gene screening process to identify potential targets of Glab and their relevance to the pathophysiology of COPD. Initially, databases such as STITCH, TCMSP, and SwissTargetPrediction were utilized to identify 182 candidate genes that Glab may target. The second phase involved databases like BATMAN-TCM, DrugBank, OMIM, and DisGeNET, from which 707 potential target genes were screened during the COPD process. Utilizing Cytoscape software, we constructed a detailed target-pathway network map that encompassed 79 intersecting target genes of Glab and COPD. Finally, further enrichment analysis of the GO and KEGG pathways revealed important pathways associated with these target genes. Among the identified pathways, the JAK/STAT signaling pathway holds a significant strategic position. This is because it is involved in regulating lung injury, and aspects such as inflammatory responses and immune responses are all influenced by this pathway. Therefore, it has received considerable attention from researchers.

The JAK/STAT signaling cascade is a communication mechanism that is crucial for normal cellular activities. This pathway is involved in a variety of biological processes, including cell growth, survival, and inflammation (O'Shea et al., 2015). This pathway, involving JAK and STAT proteins, mediates signal transduction through cell surface receptors, ultimately regulating gene expression (Bousoik & Montazeri Aliabadi, 2018; Lv et al., 2024). In pulmonary diseases, the JAK/STAT signaling pathway is involved in numerous pathological processes and plays a significant role in overall pathogenesis. For instance, in the pathogenesis of ALI, the abnormal activation of STAT3 is crucial for the formation of functional disorders in alveolar epithelial cells and pulmonary microvascular endothelial cells, and it also affects macrophage polarization, inflammatory responses, and immune responses. Moreover, research by Hua et al. (2024) has found that IL-6 can activate the JAK2/STAT3 pathway, mediating the further release of inflammatory factors, triggering a cascade-amplified inflammatory response, and participating in the occurrence and development of ALI. In COPD research, the JAK/STAT

pathway also holds significant importance. Furthermore, numerous studies have found that COPD patients can reconstruct damaged pulmonary vessels under different drug treatments and alleviate the symptoms of COPD. Liuwei Buqi Capsules (Wang et al., 2017), salmeterol combined with magnesium isoglycyrrhizinate (Yang et al., 2022) and JAK/STAT inhibitors (Verres et al., 2022). The mechanisms underlying these treatments primarily involve inhibiting the phosphorylation of JAK, STAT1, and STAT3.

The molecular docking analysis conducted in this study provides fascinating insights into the interaction between Glab and the JAK1 protein, which is a central component of the JAK-STAT signaling pathway. The regions of the JAKs interacting with the intracellular parts of the receptors include the FERM and SH2-like domains, which are responsible for the JAK association with cytokine receptors (Ferrao & Lupardus, 2017). A strong binding affinity was observed, with specific interaction sites at GLY263, GLY440, and ASN465 residues. Among these sites, GLY440 and ASN465 are located in the SH2-like domain. This suggests a potential therapeutic alliance between Glab and the modulation of JAK1 activity. We used Western blotting to verify the key interactions we obtained in the previous step. The results were consistent with our expected conclusion. CSE-stimulated 16HBE cells would enhance the expression of JAK1 and STAT1. Remarkably, treatment with Glab at various concentrations significantly mitigated this upregulation, thereby providing evidence of Glab's inhibitory influence on the JAK-STAT signaling pathway. It is worth noting that different concentrations of Glab significantly alleviated this upregulation. Glab can exert a significant inhibitory effect on the JAK-STAT signaling pathway. This biological effect shows a concentration-dependent manner. This finding implies that Glab's protective effects in COPD may be mediated through the JAK1/STAT1 pathway and that its influence on cell viability, apoptosis, and inflammation is maximized when the pathway is not otherwise disrupted.

Despite the robust findings, the study acknowledges limitations inherent in its design and execution. Although these *in vitro* experiments simulate certain representative *in vivo* activities, due to the complexity of the life system's operation, this model is currently unable to precisely replicate all *in vivo* life activities. The use of a single cell line, though representative, might not reflect the heterogeneity of cellular responses in actual COPD patients. Additionally, while the study identifies the JAK1/STAT1 pathway as a potential target for Glab intervention, the broader implications of this interaction within the intricate network of pulmonary inflammation require further exploration. Lastly, while the study presents Glab as a promising candidate for COPD treatment, the specific dosage, long-term effects, and potential side effects in clinical settings remain to be determined. Future research should aim to bridge these gaps, ensuring a well-rounded understanding of Glab's therapeutic potential and its place in COPD management strategies.

Conclusion

Overall, this study confirmed that the inflammatory response of 16HBE cells stimulated by CSE is one of the main causes of cell damage. Meanwhile, Glab can specifically inhibit the phosphorylation of proteins in the JAK1/STAT1 pathway, alleviate the inflammatory response, and play a therapeutic role in the inflammatory damage of 16HBE cells. These findings not only suggest Glab's potential as an effective modulator of inflammatory processes but also emphasize the critical role of targeting the JAK1/STAT1 pathway in formulating therapeutic approaches for COPD.

Abbreviations

16HBE: Human bronchial epithelial cells; ALI: Acute lung injury; ANOVA: Analysis of variance; ARDS: Acute respiratory distress syndrome; CCK-8: Cell Counting Kit-8; cDNA: Complementary deoxyribose nucleic acid; COPD: Chronic obstructive pulmonary disease; CSE: Cigarette smoke extract; DMEM: Dulbecco's Modified Eagle Medium; DMSO: Dimethyl sulfoxide; ECL: Enhanced chemiluminescence; ELISA: Enzyme-linked immunosorbent assay; ERK: Extracellular signal-regulated kinase; FITC: Fluorescein isothiocyanate; Glab: Glabridin; GO: Gene Ontology; HRP: Horseradish peroxidase; IL-6: Interleukin-6; IL-1β: Interleukin-1β; IL-8: Interleukin-8; JAK1: Janus kinase 1; KEGG: Kyoto Encyclopedia of Genes and Genomes; OD: Absorbance; OGD/R: Oxygen-glucose deprivation/reoxygenation; p38MAPK: Mitogen-activated protein kinase 14; PDB: Protein Data Bank; PI: Propidium iodide; PVDF: Polyvinylidene fluoride; qRT-PCR: Quantitative real-time polymerase chain reaction; SPSS: Statistic Package for Social Science; STAT1: Signal transducer and activator of transcription 1; TCMSP: Traditional Chinese Medicine Systems Pharmacology Database and Analysis Platform; TNF-α: Tumor necrosis factor-α.

Authors' Contributions

Weiwei Yuan: Conceptualization, Formal analysis, Methodology, Validation.
Hongtao Tan: Conceptualization, Formal analysis, Methodology, Validation.
Huihui Li: Formal analysis, Data curation, Investigation.
Junxian Chen: Data curation, Investigation, Writing – original draft, Writing – review & editing.
Jun Qiu: Formal analysis, Funding acquisition, Investigation, Project administration, Resources.

Declaration of Conflicting Interests

The authors declared no potential conflicts of interest with respect to the research, authorship, and/or publication of this article.

Ethical Approval and Informed Consent

Not applicable.

Funding

The authors disclosed receipt of the following financial support for the research, authorship, and/or publication of this article: This work

was supported by 2023 Science and Research Project of Traditional Chinese Medicine Bureau of Guangdong Province (Grant Number 20232137); 2024 Science and Research Project of Traditional Chinese Medicine Bureau of Guangdong Province (No.20241334); and 2022 Medical and Health Field Science Technology Plan Project in Huizhou City (No.2022CZ010163).

ORCID iD

Jun Qiu https://orcid.org/0009-0001-8717-0824

References

Aslani, M. R., Abdollahi, N., Matin, S., Zakeri, A., & Ghobadi, H. (2023). Effect of crocin of *Crocus sativus* L. on serum inflammatory markers (IL-6 and TNF-alpha) in chronic obstructive pulmonary disease patients: A randomised, double-blind, placebo-controlled trial. *The British Journal of Nutrition*, *130*(3), 446–453. https://doi.org/10.1017/S0007114522003397

Bousoik, E., & Montazeri Aliabadi, H. (2018). "Do We Know Jack" about JAK? A closer look at JAK/STAT signaling pathway. *Frontiers in Oncology*, *8*, 287. https://doi.org/10.3389/fonc.2018.00287

Christenson, S. A., Smith, B. M., Bafadhel, M., & Putcha, N. (2022). Chronic obstructive pulmonary disease. *The Lancet*, *399*(10342), 2227–2242. https://doi.org/10.1016/S0140-6736(22)00470-6

Dang, X., He, B., Ning, Q., Liu, Y., Guo, J., Niu, G., & Chen, M. (2020). Alantolactone suppresses inflammation, apoptosis and oxidative stress in cigarette smoke-induced human bronchial epithelial cells through activation of Nrf2/HO-1 and inhibition of the NF-kappaB pathways. *Respiratory Research*, *21*(1), 95. https://doi.org/10.1186/s12931-020-01358-4

Deveci, Y., Deveci, F., Ilhan, N., Karaca, I., Turgut, T., & Muz, M. H. (2010). Serum ghrelin, IL-6 and TNF-alpha levels in patients with chronic obstructive pulmonary disease. *Tuberkuloz ve Toraks*, *58*(2), 162–172.

Ferrao, R., & Lupardus, P. J. (2017). The Janus kinase (JAK) FERM and SH2 domains: Bringing specificity to JAK-receptor interactions. *Frontiers in Endocrinology*, *8*, 71. https://doi.org/10.3389/fendo.2017.00071

Gao, W., Li, L., Wang, Y., Zhang, S., Adcock, I. M., Barnes, P. J., Huang, M., & Yao, X. (2015). Bronchial epithelial cells: The key effector cells in the pathogenesis of chronic obstructive pulmonary disease? *Respirology*, *20*(5), 722–729. https://doi.org/10.1111/resp.12542

Guo, Q., Wu, S., Liang, W., Tan, J., Liu, X., Yuan, Y., Li, X., & Zhao, H. (2022). Glabrol impurity exacerbates glabridin toxicity in zebrafish embryos by increasing myofibril disorganization. *Journal of Ethnopharmacology*, *287*, Article 114963. https://doi.org/10.1016/j.jep.2021.114963

He, S., Wu, L., Sun, H., Wu, D., Wang, C., Ren, X., Shao, Q., York, P., Tong, J., Zhu, J., Li, Z., & Zhang, J. (2022). Antioxidant biodegradable covalent cyclodextrin frameworks as particulate carriers for inhalation therapy against acute lung injury. *ACS Applied Materials and Interfaces*, *14*(34), 38421–38435. https://doi.org/10.1021/acsami.2c05220

Hizawa, N. (2024). Common pathogeneses underlying asthma and chronic obstructive pulmonary disease—Insights from genetic studies. *International Journal of Chronic Obstructive Pulmonary Disease*, *19*, 633–642. https://doi.org/10.2147/COPD.S441992

Hua, M., Gao, P., Fang, F., Su, H., & Song, C. (2024). IL-6 enhances the phagocytic function of mouse alveolar macrophages by activating the JAK2/STAT3 signaling pathway. *Xi Bao Yu Fen Zi Mian Yi Xue Za Zhi*, *40*(1), 13–18.

Kang, J. S., Yoon, Y. D., Cho, I. J., Han, M. H., Lee, C. W., Park, S.-K., & Kim, H. M. (2005). Glabridin, an isoflavan from licorice root, inhibits inducible nitric-oxide synthase expression and improves survival of mice in experimental model of septic shock. *The Journal of Pharmacology and Experimental Therapeutics*, *312*(3), 1187–1194. https://doi.org/10.1124/jpet.104.077107

Kapellos, T. S., Baßler, K., Fujii, W., Nalkurthi, C., Schaar, A. C., Bonaguro, L., Pecht, T., Galvao, I., Agrawal, S., Saglam, A., Dudkin, E., Frishberg, A., de Domenico, E., Horne, A., Donovan, C., Kim, R. Y., Gallego-Ortega, D., Gillett, T. E., & Schultze, J. L. (2023). Systemic alterations in neutrophils and their precursors in early-stage chronic obstructive pulmonary disease. *Cell Reports*, *42*(6), Article 112525. https://doi.org/10.1016/j.celrep.2023.112525

Kodaka, N., Nakano, C., Oshio, T., Hirouchi, T., Yamada, Y., & Matsuse, H. (2023). Effects of dupilumab for asthma-chronic obstructive pulmonary disease overlap. *Iranian Journal of Allergy, Asthma, and Immunology*, *22*(2), 212–216. https://doi.org/10.18502/ijaai.v22i2.12683

Li, T., Li, H., Xia, W., Li, M., Niu, Y., & Fu, X. (2023). Investigation of the effects of glabridin on the proliferation, apoptosis and migration of the human colon cancer cell lines SW480 and SW620 and its mechanism based on reverse virtual screening and proteomics. *Oxidative Medicine and Cellular Longevity*, 2023, Article 1117431. https://doi.org/10.1155/2023/1117431

Lv, Y., Qi, J., Babon, J. J., Cao, L., Fan, G., Lang, J., Zhang, J., Mi, P., Kobe, B., & Wang, F. (2024). The JAK-STAT pathway: From structural biology to cytokine engineering. *Signal Transduction and Targeted Therapy*, *9*(1), 221. https://doi.org/10.1038/s41392-024-01934-w

O'Shea, J. J., Schwartz, D. M., Villarino, A. V., Gadina, M., McInnes, I. B., & Laurence, A. (2015). The JAK-STAT pathway: Impact on human disease and therapeutic intervention. *Annual Review of Medicine*, *66*, 311–328. https://doi.org/10.1146/annurev-med-051113-024537

Parlar, A., Arslan, S. O., & Çam, S. A. (2020). Glabridin alleviates inflammation and nociception in rodents by activating BK(Ca) channels and reducing NO levels. *Biological and Pharmaceutical Bulletin*, *43*(5), 884–897. https://doi.org/10.1248/bpb.b20-00038

Ran, N., Pang, Z., Gu, Y., Pan, H., Zuo, X., Guan, X., Yuan, Y., Wang, Z., Guo, Y., Cui, Z., & Wang, F. (2019). An updated overview of metabolomic profile changes in chronic obstructive pulmonary disease. *Metabolites*, *9*(6), Article 111. https://doi.org/10.3390/metabo9060111

Ritchie, A. I., & Wedzicha, J. A. (2020). Definition, causes, pathogenesis and consequences of chronic obstructive pulmonary disease exacerbations. *Clinics in Chest Medicine*, *41*(3), 421–438. https://doi.org/10.1016/j.ccm.2020.06.007

Song, H., Jiang, L., Yang, W., Dai, Y., Wang, Y., Li, Z., Liu, P., & Chen, J. (2023). Cryptotanshinone alleviates lipopolysaccharide and cigarette smoke-induced chronic obstructive pulmonary disease in mice via the Keap1/Nrf2 axis. *Biomedicine and Pharmacotherapy*, *165*, Article 115105. https://doi.org/10.1016/j.biopha.2023.115105

Tan, H., Chen, J., Li, Y., Li, Y., Zhong, Y., Li, G., Liu, L., & Li, Y. (2022). Glabridin, a bioactive component of licorice, ameliorates diabetic nephropathy by regulating ferroptosis and the VEGF/Akt/ERK pathways. *Molecular Medicine*, *28*(1), 58. https://doi.org/10.1186/s10020-022-00481-w

Upadhyay, P., Wu, C.-W., Pham, A., Zeki, A. A., Royer, C. M., Kodavanti, U. P., Takeuchi, M., Bayram, H., & Pinkerton, K. E. (2023). Animal models and mechanisms of tobacco smoke-induced chronic obstructive pulmonary disease (COPD). *Journal of Toxicology and Environmental Health. Part B, Critical Reviews*, *26*(5), 275–305. https://doi.org/10.1080/10937404.2023.2208886

Verres, Y., da Silva, C. O., Aljebawi, B., Bodin, A., Barreto, E., Lagente, V., & Victoni, T. (2022). Impact of JAK/STAT inhibitors on human monocyte-derived-macrophages stimulated by cigarette smoke extract and lipopolysaccharide. *Clinical and Experimental Pharmacology and Physiology*, *49*(11), 1187–1196. https://doi.org/10.1111/1440-1681.13705

Wahab, S., Annadurai, S., Abullais, S. S., Das, G., Ahmad, W., Ahmad, M. F., Kandasamy, G., Vasudevan, R., Ali, M. S., & Amir, M. (2021). *Glycyrrhiza glabra* (licorice): A comprehensive review on its phytochemistry, biological activities, clinical evidence and toxicology. *Plants*, *10*(12), Article 2751. https://doi.org/10.3390/plants10122751

Wang, C., Ding, H., Tang, X., Li, Z., & Gan, L. (2017). Effect of Liuweibuqi capsules in pulmonary alveolar epithelial cells and COPD through JAK/STAT pathway. *Cellular Physiology and Biochemistry*, *43*(2), 743–756. https://doi.org/10.1159/000481558

Weng, J., Wang, Y., Tan, Z., Yuan, Y., Huang, S., Li, Z., Li, Y., Zhang, L., & Du, Z. (2024). Glabridin reduces neuroinflammation by modulating inflammatory signals in LPS-induced *in vitro* and *in vivo* models. *Inflammopharmacology*, *32*(2), 1159–1169. https://doi.org/10.1007/s10787-023-01424-5

Yang, Y., Huang, L., Tian, C., & Qian, B. (2022). Efficacy of salmeterol and magnesium isoglycyrrhizinate combination treatment in rats with chronic obstructive pulmonary disease. *Scientific Reports*, *12*(1), Article 12334. https://doi.org/10.1038/s41598-022-16775-2

Zhan, L., Tian, X., Lin, J., Peng, X., & Zhao, G. (2023). Glabridin inhibits *Aspergillus fumigatus* growth and alleviate inflammation mediated by Dectin-2 and NLRP3 inflammasome. *Current Eye Research*, *48*(4), 348–356. https://doi.org/10.1080/02713683.2022.2164779

Zhang, L. P., & Li, J. G. (2016). Glabridin reduces lipopolysaccharide-induced lung injury in rats by inhibiting p38 mitogen activated protein kinase/extracellular regulated protein kinases signaling pathway. *Zhonghua Yi Xue Za Zhi*, *96*(48), 3893–3897. https://doi.org/10.3760/cma.j.issn.0376-2491.2016.48.009

Zhang, M.-Y., Jiang, Y.-X., Yang, Y.-C., Liu, J.-Y., Huo, C., Ji, X.-L., & Qu, Y.-Q. (2021). Cigarette smoke extract induces pyroptosis in human bronchial epithelial cells through the ROS/NLRP3/caspase-1 pathway. *Life Sciences*, *269*, Article 119090. https://doi.org/10.1016/j.lfs.2021.119090

Zhang, L., Zhang, H., Gu, J., Xu, W., Yuan, N., Sun, J., & Li, H. (2022). Glabridin inhibits liver fibrosis and hepatic stellate cells activation through suppression of inflammation and oxidative stress by activating PPARgamma in carbon tetrachloride-treated mice. *International Immunopharmacology*, *113*(B), Article 109433. https://doi.org/10.1016/j.intimp.2022.109433

Zhang, L.-P., Zhao, Y., Liu, G.-J., Yang, D.-G., Dong, Y.-H., & Zhou, L.-H. (2017). Glabridin attenuates lipopolysaccharide-induced acute lung injury by inhibiting p38MAPK/ERK signaling pathway. *Oncotarget*, *8*(12), 18935–18942. https://doi.org/10.18632/oncotarget.14277